

Analysis of Inscribed Hexagonal Slot Loaded Antenna for Short Range RFID Reader Applications

Rupanita Das¹, Tanmaya K. Das², Ajay K. Yadav¹, Harish C. Mohanta³,
Abdul K. M. Zakir Hossain^{4,*}, and Ahmed J. A. Al-Gburi^{4,*}

¹Department of ECE, C. V. Raman Global University, Bhubaneswar, Odisha, India

²School of Electronics Engineering, Vellore Institute of Technology, Vellore, Tamil Nadu, India

³Department of ECE, Centurion University of Technology and Management, India

⁴Center for Telecommunication Research & Innovation (CeTRI), Faculty of Electronics and Computer Technology and Engineering, Universiti Teknikal Malaysia Melaka (UTeM), Jalan Hang Tuah Jaya, Durian Tunggal 76100, Melaka, Malaysia

ABSTRACT: This article introduces an inscribed hexagonal-slot square patch antenna developed in the field of RFID technology for reader applications. The proposed structure is energized with one feeding element. This study proposes a high-gain microstrip antenna for ISM band applications at 5.8 GHz. FR4 material is utilized in the design and fabrication of the antenna. The resulting design achieves a -10 dB impedance bandwidth of around 3.6% in the ISM band. The proposed design is compact in comparison to several contemporary designs and has dimensions of $0.43\lambda \times 0.43\lambda \times 0.03\lambda$ ($\lambda =$ wavelength at 5.8 GHz). The measurement reveals that the antenna can operate across the frequency band 5.67 GHz–5.88 GHz having a maximum gain value of 4.58 dBi at 5.77 GHz. The satisfaction of the propagation test in different environments and the reading distance value of 2.81 cm at the ISM band supports the application of the structure as a short-range RFID reader.

1. INTRODUCTION

Radio frequency identification (RFID) is one of the significant methods in the recent developments of short-range wireless technology. This technology uses inductive or electromagnetic coupling to automatically acquire data about a physical object without a need to touch or see the data carrier [1]. A chip attached to an electronic device is known as a data carrier. Fig. 1 demonstrates the basic block diagram representation of an RFID system. The information is transmitted to the antenna (known as a tag or transponder). RFID has intrinsic benefits, such as the absence of a line-of-sight requirement, database portability, and resistance to adverse environmental conditions [2]. The Federal Communications Commission (FCC) established ISM (Industrial, Scientific, and Medical) bands in the United States, and most other nations have designated ISM bands (2.4–2.48 GHz, 5.72–5.87 GHz) for unlicensed usage. It is a crucial frequency range that is starting to be extensively used [3]. The frequency range allocated for RFID technology is listed in Table 1 [1]. RFID technology has a broad range of applications in different sectors such as healthcare, identification, logistics, and security [4]. The tracking of goods has become critical to maintaining transparency in the logistics between customers, middlemen, and organizers. Technology enables real-time identification, tracking, and tracing of essential healthcare assets (like wheelchairs and infusion pumps) to encourage better management of these resources [5]. All these

RFID-enabled scenarios possess the capabilities to enable new value creation in healthcare service innovation [6]. Healthcare stakeholders can utilize technology to track and trace items from the collection location to the healthcare facility, as well as identify blood bags at the collecting station, which is a step in the patient blood collection and transfusion process.

TABLE 1. Frequency bands assigned for RFID applications.

| Frequency Band | Range |
|------------------------------------|--------------------------------|
| LF: Low frequency | 125–134 kHz |
| HF: High frequency | 13.56 MHz |
| UHF: Ultra-high frequency | 840–960 MHz |
| Microwave frequency (ISM bands) | 2.4–2.48 GHz, 5.72–5.87 GHz |

Microstrip antennas are used as RFID readers in various applications [7]. The low profile, effective adaptability to planar and nonplanar surfaces, and mechanical robustness, when they are placed on stiff surfaces, are the reasons for the popularity of microstrip antennas [8]. Mainly two types of planar antennas are used for RFID applications, i.e., linearly polarized (LP) [9] and circularly polarized (CP) [10] antennas. The linearly polarized antenna can be advantageous in providing improved cross-polarization and lowering the cost of the overall antenna system. In some scenarios, it also reduces required transmission power approximately by 50% [11]. In certain internet of things (IoT)-based applications, compared to the contemporary CP designs, these reduced energy requirements can be beneficial [11].

* Corresponding authors: Abdul Kayum Muhammad Zakir Hossain (zakir@utem.edu.my) and Ahmed Jamal Abdullah Al-Gburi (ahmedjamal@ieec.edu.my).

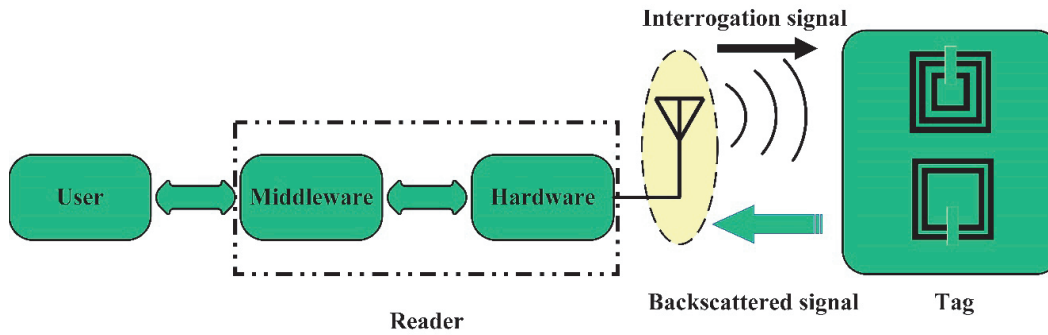


FIGURE 1. Block diagram of an RFID system.

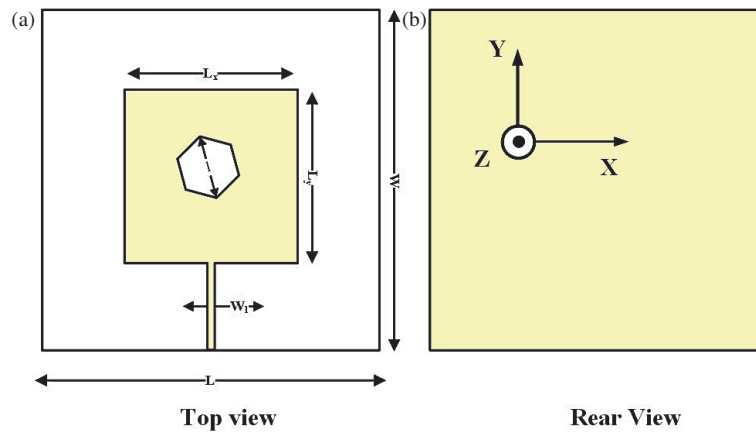


FIGURE 2. Geometrical representation of suggested work.

Miniaturization is one of the most important factors of antennas for wireless communication devices. Slot antennas are ideal for these applications because of their simple structure [12]. The basic component in a slot antenna includes a narrow, straight slot which is electromagnetically fed by a microstrip transmission line. The pattern of the straight slots can be altered to satisfy a reduced dimension requirement. The 300 MHz to 30 GHz frequency range mostly utilized the operating band for slot antennas [13]. It uses the UHF and SHF frequency ranges.

This research demonstrates a microstrip line-fed inscribed hexagonal slot-loaded square-shaped RFID reader. The linearly polarized RFID reader antenna shows a maximum gain of 4.58 dBi at 5.77 GHz. The antenna has a stable omnidirectional radiation pattern. An antenna prototype has been designed and fabricated. Along with this, analytical modeling is provided to understand the operation of the suggested antenna. The propagation test signifies the operability of the proposed work as an RFID reader antenna in different environments. The read range value also shows its potential as a reader antenna.

The article is structured as follows. Section-2 presents the proposed antenna's geometry and design. It also describes the parametric analysis to comprehend how different characteristics affect the performance and how effectively the design works. Analytical modeling and the comparison of full-wave simulation with model outcomes are covered in Section 3. The analysis of the suggested design's results is presented in Sec-

tion 4. Performance analysis and a comparison with related literature are shown in Section 5, followed by the conclusion of the study in Section 6.

2. GEOMETRY AND DESIGN OF READER ANTENNA

2.1. Structure

The suggested antenna (Fig. 2) contains a square-shaped patch with dimension $L_x \times L_y$. The LP antenna is placed over a low-cost FR4 epoxy substrate ($\epsilon_r = 4.4$, $\tan \delta = 0.02$) having dimensions $L \times W \times h_s$. The structure has a full ground plane at the backside of the substrate of dimensions $L \times W$. The radiator has an inscribed hexagonal slot rotated anticlockwise with an angle of 15° around the Z-axis.

The incorporation of a slot provides better gain, and the radiator is fed by microstrip line feeding with an input impedance of 50Ω . The full-wave simulation is accomplished by ANSYS HFSS version 19 EM simulator. The geometrical details are shown in Table 2.

TABLE 2. The proposed antenna's design dimensions.

| | | | | | | | |
|-------|---------|-------|---------|-------|--------|-------|--------|
| L_x | 11.2 mm | L_y | 11.2 mm | l | 1.4 mm | W_1 | 0.5 mm |
| W | 22.4 mm | L | 22.4 mm | h_s | 0.5 mm | | |

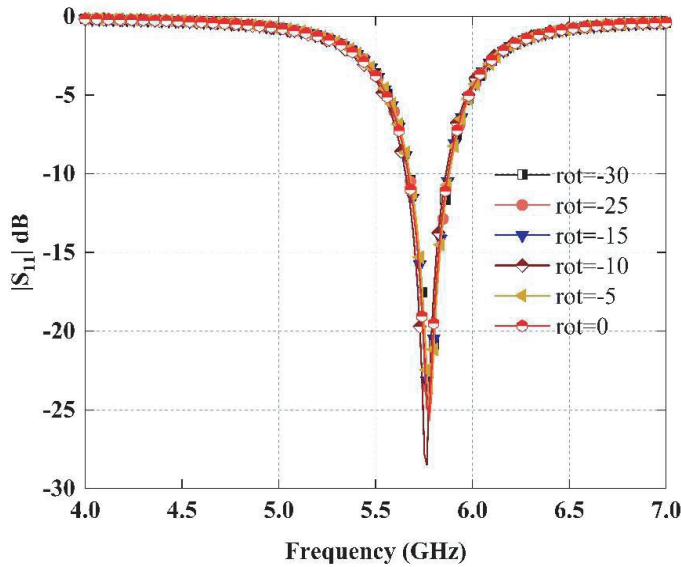


FIGURE 3. Variation of reflection coefficients with rotation angle of hexagonal slot (*rot*).

TABLE 3. The comparison of the antenna’s gain with different slots resonating at 5.77 GHz.

| Shapes | Hexagonal | Circular | Rectangular | Elliptical |
|------------|-----------|----------|-------------|------------|
| Gain (dBi) | 4.58 | 4.55 | 4.53 | 4.51 |

In the simulation environment, after designing the square patch, various shapes of the slots were examined. The realized gain value of all the structures resonating at 5.77 GHz is presented in Table 3. This provides insight for choosing the hexagonal slot in the proposed structure. After conducting parametric analysis at various rotation angles (0° , -5° , -10° , -15° , -25° , and -30°), it was determined that the $|S_{11}|$ values of all the structures are less than -10 dB within the frequency range of 5.67 GHz to 5.88 GHz resonating at 5.77 GHz. The corresponding gains are 4.52 GHz, 4.54 GHz, 4.56 GHz, 4.58 GHz, 4.56 GHz, and 4.54 GHz, respectively. It was noted that the $|S_{11}|$ values and gain are optimal at an angle of -15° . The variation of reflection coefficients with different rotation angles is illustrated in Fig. 3.

2.2. Parametric Analysis

The proposed design has some important parameters which affect the response of the antenna. To understand these effects, a parametric study was conducted in a full-wave simulation environment by using ANSYS HFSS. Fig. 3 depicts the variation in reflection coefficients at different rotation angles. As shown in the figure, the response shows better results at -15° . The parameter, such as hexagonal slot width (l), is varied, and the corresponding $|S_{11}|$ response is analyzed. Fig. 4 depicts the variation in reflection coefficients according to l . As shown in the figure, the response shows better impedance matching for $l = 1.4$ mm.

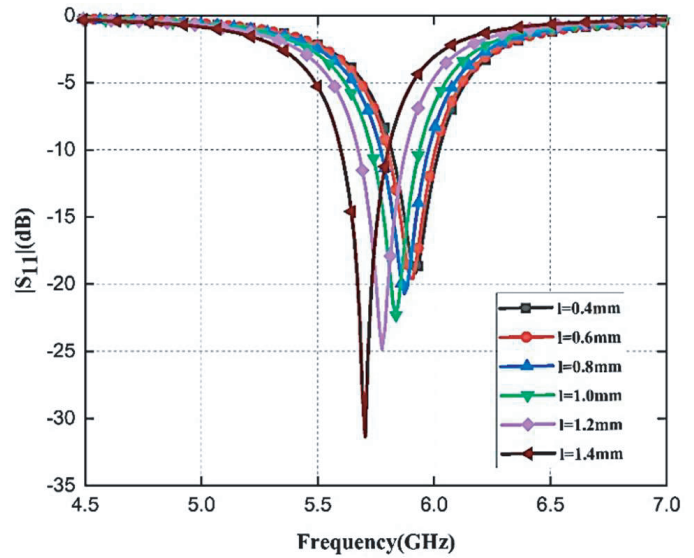


FIGURE 4. Variation of reflection coefficients with “ l ”.

2.3. Surface Current Analysis

The surface current distribution plot (Fig. 5) can be utilized to further describe how well the suggested design operates. The plot shows the change in surface currents (magnitude — Fig. 5(a), vector — Fig. 5(b)) at 5.8 GHz in the simulation environment. It shows that at this frequency, the surface current is the greatest across the radiator. This meets the requirement of resonant frequency concerning the electrical length.

3. ANALYTICAL MODELING

The suggested LP antenna can be analyzed using lumped elements to produce an electrical equivalent circuit. Fig. 6 shows that the suggested antenna comprises series connected one-stage parallel RLC circuits and LC circuit. The RLC tank circuit is due to the microstrip patch antenna, and the slot can be modeled by using a series connected LC circuit [14]. The values of the LP antenna’s lumped elements are determined by the Advanced Design System (ADS) software optimization tool and are displayed in Table 4.

TABLE 4. The lumped element value of the proposed antenna.

| Z_n | Z_0 | Z_1 |
|-------------------|-------|-------|
| $R_n (\Omega)$ | | 62 |
| $L_n (\text{nH})$ | 0.645 | 0.158 |
| $C_n (\text{pF})$ | 0.32 | 4.53 |

For $|S_{11}|$ and input impedance (Z_{in}) responses, a comparison is made between the simulation (HFSS) results and the analytical model. Fig. 7 shows that the $|S_{11}|$ values of the equivalent circuit (both with and without slot) are < -10 dB from 5.67 GHz to 5.88 GHz. The Z_{in} in Fig. 8 represents the input impedance value of the final design. It also shows resonance at 5.77 GHz with good impedance matching in the

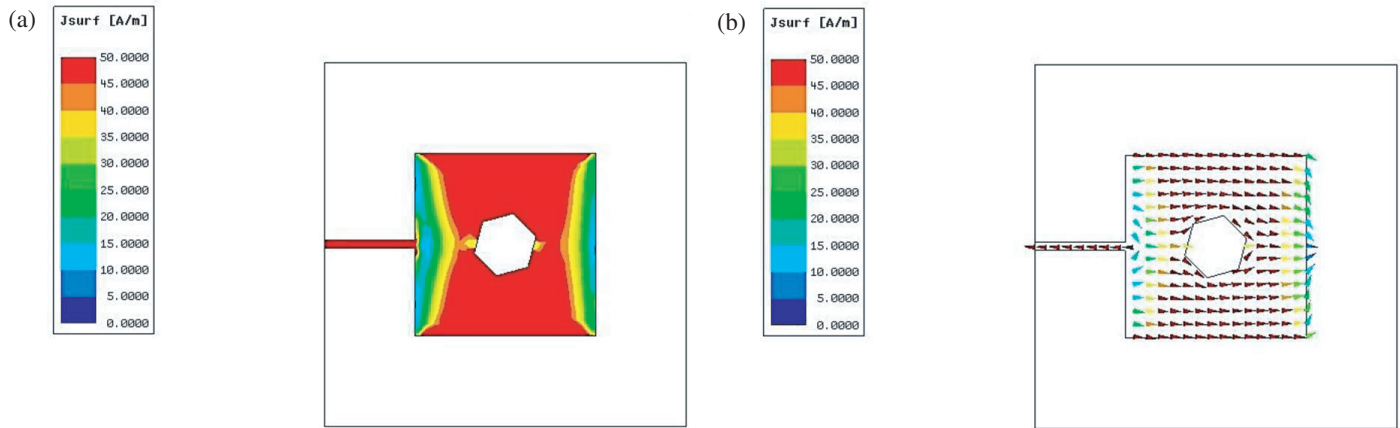


FIGURE 5. Surface current (magnitude and vector) plot.

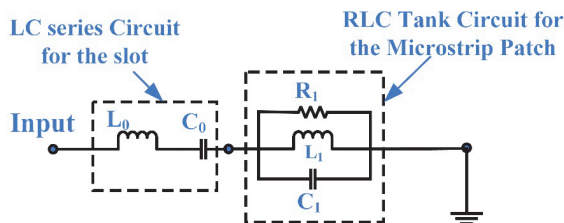


FIGURE 6. The electrical equivalent circuit of the suggested design employing lumped parts.

5.67 GHz–5.88 GHz frequency region. The outcomes of both, i.e., HFSS and model, are well correlated. lobe with FBR > 13 dB for the operating band.

4. MEASUREMENT RESULTS AND ANALYSIS

The suggested design is made on a low-cost FR4 material, and the prototype is presented in Fig. 9. Fig. 10 depicts a measurement setup inside an anechoic chamber. The $|S_{11}|$ response plot of the LP antenna is given in Fig. 11. The $|S_{11}|$ measurement was accomplished using the performance network analyzer (PNA: N5222B). It indicates the resonance at 5.77 GHz in the range of 5.67 GHz–5.88 GHz, with $|S_{11}|$ being < -10 dB in this range. The figure makes it clear that the resonant frequency in measured response fairly matches the outcomes of the simulation. A slight shift in resonant frequency could be the result of the soldering effect.

The 2-D radiation plots in the two perpendicular planes, i.e., for $\phi = 0^\circ, 90^\circ$ at 5.77 GHz are demonstrated in Fig. 12. The radiation patterns show that within a broad beamwidth of approximately 120° , about 30 dB lower value is present at cross-polarization (cross-pol) value than co-polarization (co-pol) in both planes. Fig. 13 depicts the simulated 3-D radiation patterns for the suggested antenna at a frequency of 5.77 GHz. The plot makes it clear that the antenna has an omnidirectional pattern.

Figure 14 exhibits the realized gain variation as a function of frequency. The outcomes of simulation and measurement for the intended frequency range of 5.67 GHz to 5.88 GHz agree extremely well. It demonstrates that in the whole operating frequency range, the gain is more than a value of 4 dBi, and the

peak value at resonance frequency is about 4.58 dBi. The simulated front-to-back ratio (FBR) response is shown in Fig. 15. It shows a reduced back

5. PERFORMANCE ANALYSIS IN DIFFERENT ENVIRONMENTS

5.1. Propagation Test

Since the suggested structure is intended for RFID reader applications, there is a chance that some nonconducting obstructions (as an interfering medium between the tag and reader) may hamper the performance. For this purpose, a test is performed (propagation test) to comprehend the impact of these mediums, like fabric and cardboard. The propagation test is conducted in a simulation environment under two different conditions, namely: (1) a fabric covering ($\epsilon_r = 1.8, \tan \delta = 0.016$), and (2) a cardboard covering ($\epsilon_r = 1.42, \tan \delta = 0.043$) [10]. Fig. 16 and Fig. 17 show simulated and measured propagation tests: $|S_{11}|$ versus frequency response in various environments (cloth and cardboard). It also demonstrates that the variation in $|S_{11}|$ of the proposed design in free space (Fig. 11) closely matches the responses with various non-conducting mediums. The test is also conducted to analyze 2-D radiation characteristics at 5.77 GHz in an environment under two different conditions, namely: (1) a fabric covering, and (2) a cardboard covering for the two perpendicular planes, i.e., for $\phi = 0^\circ, 90^\circ$. Fig. 18 and Fig. 19 show simulated and measured radiation patterns for cloth and cardboard. The radiation response depicts that the cross-pol elements are less than the co-pol elements by 15 dB. It is also found that the simulated and measured results are well matched. Hence, the design can be successfully allocated as a reader in RFID technology.

5.2. Read Range Analysis

The read range of an antenna is one of the key features of any RFID reader. This section is intended to calculate the read range and analyze its behavior concerning frequency variation. The

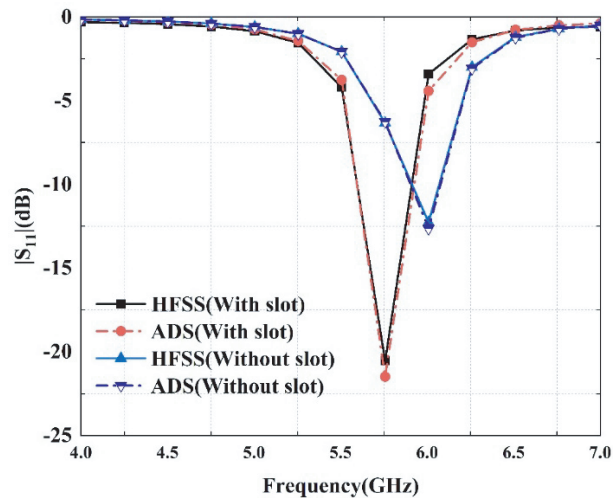


FIGURE 7. Comparison between the $|S_{11}|$ values obtained from the simulation and analytical model.

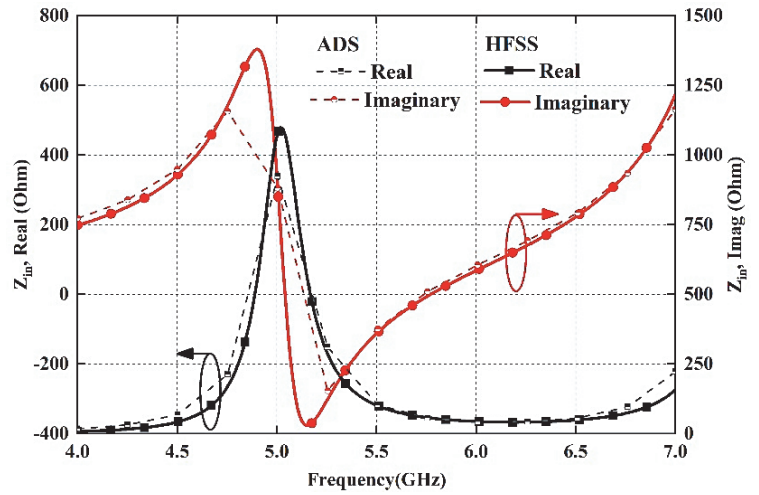


FIGURE 8. Comparison between the impedance values obtained from the simulation and analytical model.

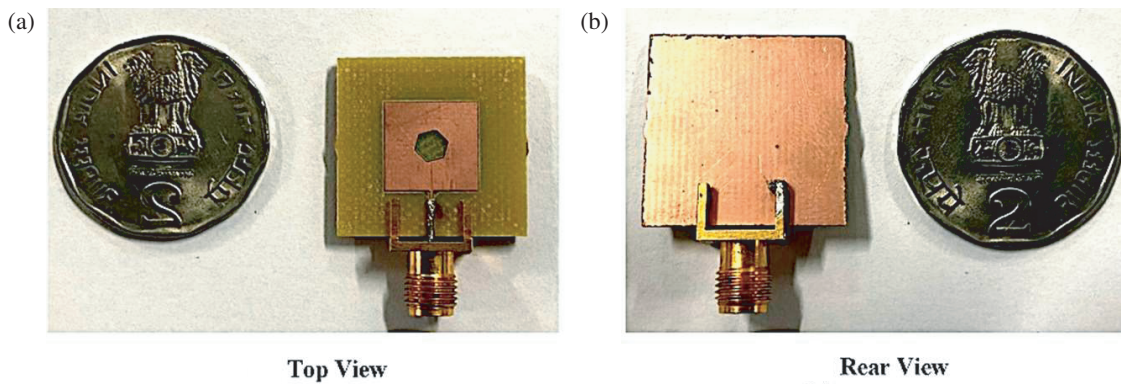


FIGURE 9. Fabricated prototype of the suggested work.

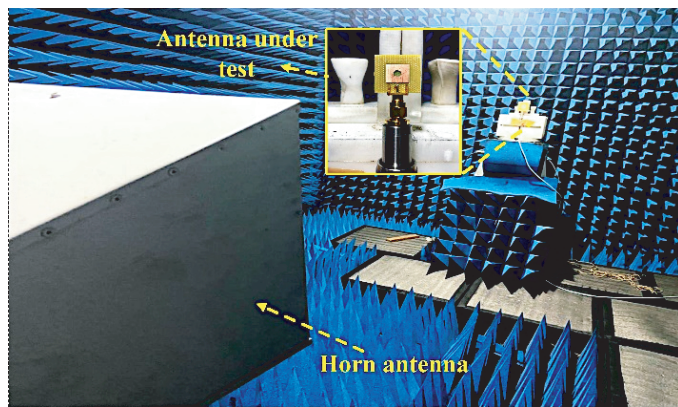


FIGURE 10. Setting up measurements within the anechoic chamber.

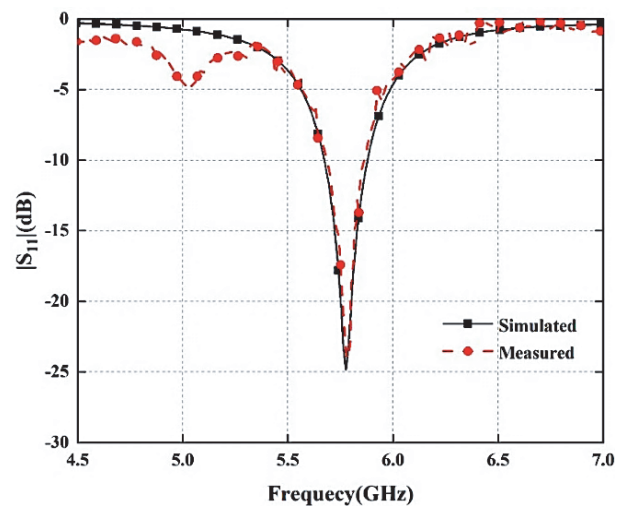


FIGURE 11. The suggested antenna's frequency response as a function of $|S_{11}|$.

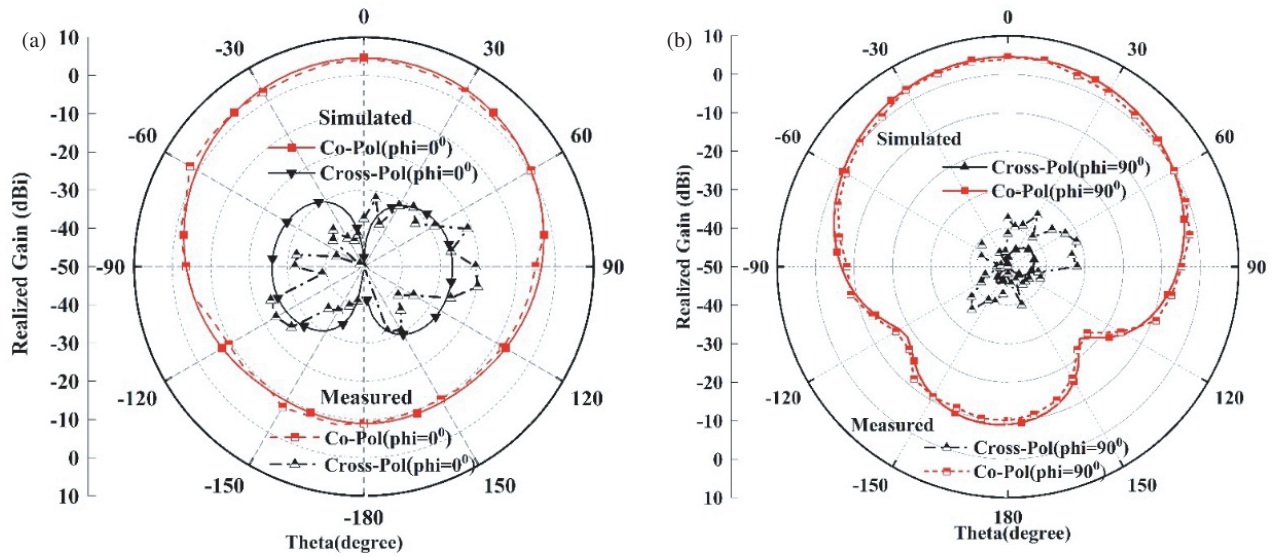


FIGURE 12. The 2-D radiation plots of the suggested antenna at 5.77 GHz. (a) $\phi = 0^\circ$, (b) $\phi = 90^\circ$.

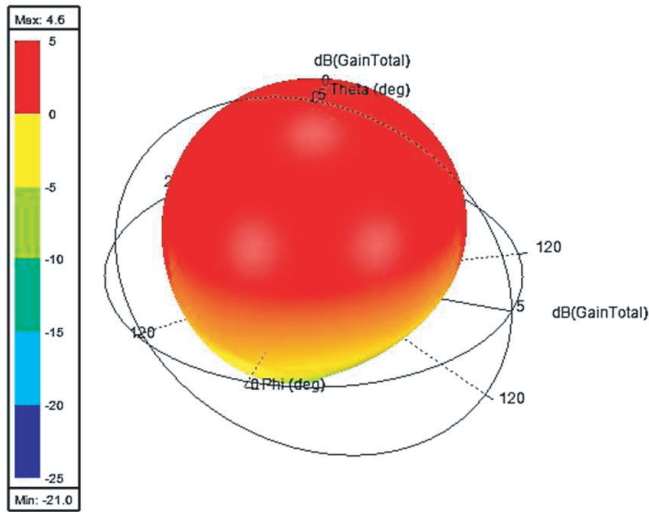


FIGURE 13. The proposed antenna's 3D-radiation pattern.

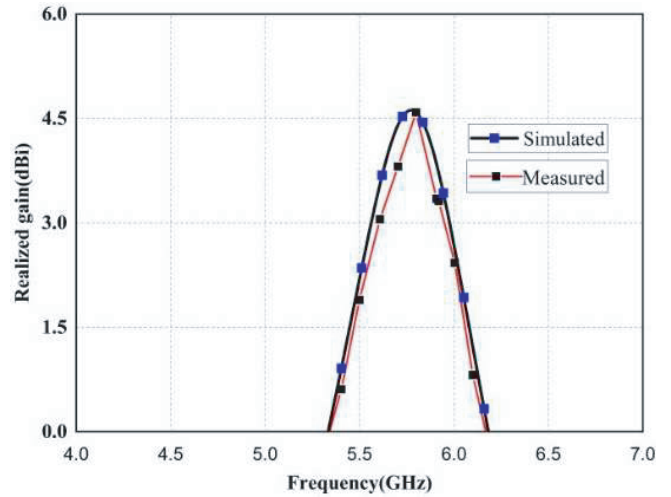


FIGURE 14. The realized gain vs. frequency response of the suggested antenna.

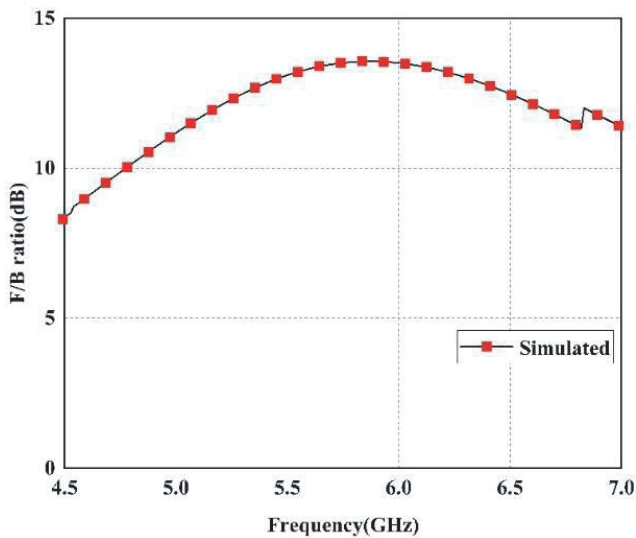


FIGURE 15. The simulated F/B ratio plot of the suggested antenna.

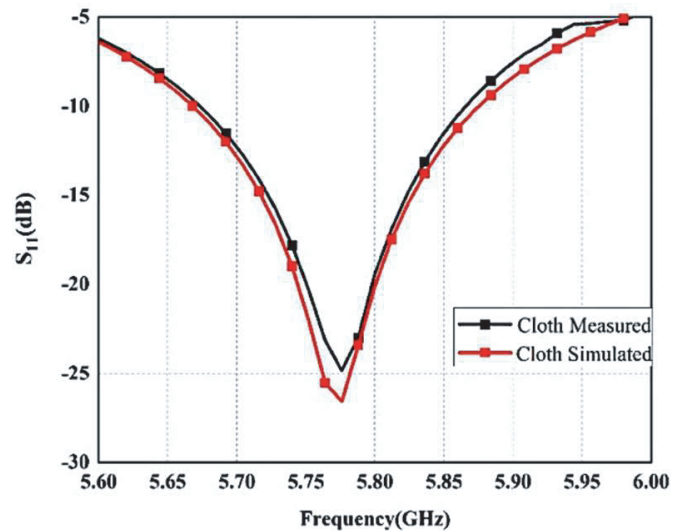


FIGURE 16. Simulated and measured antenna propagation test: $|S_{11}|$ versus frequency response in cloth environments.

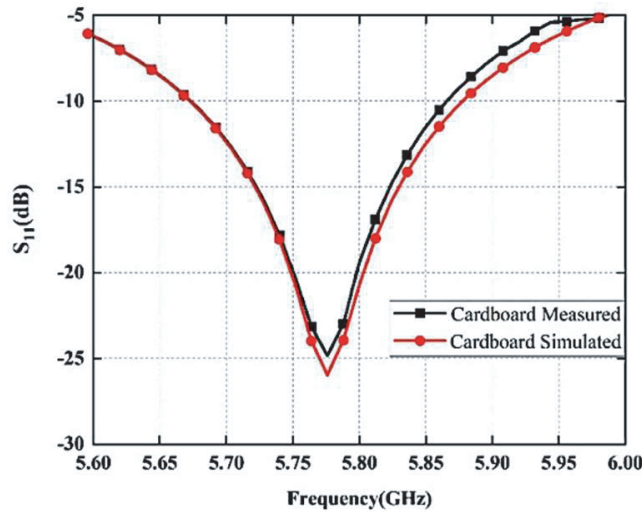


FIGURE 17. Simulated and measured antenna propagation test: $|S_{11}|$ versus frequency response in cardboard environments.

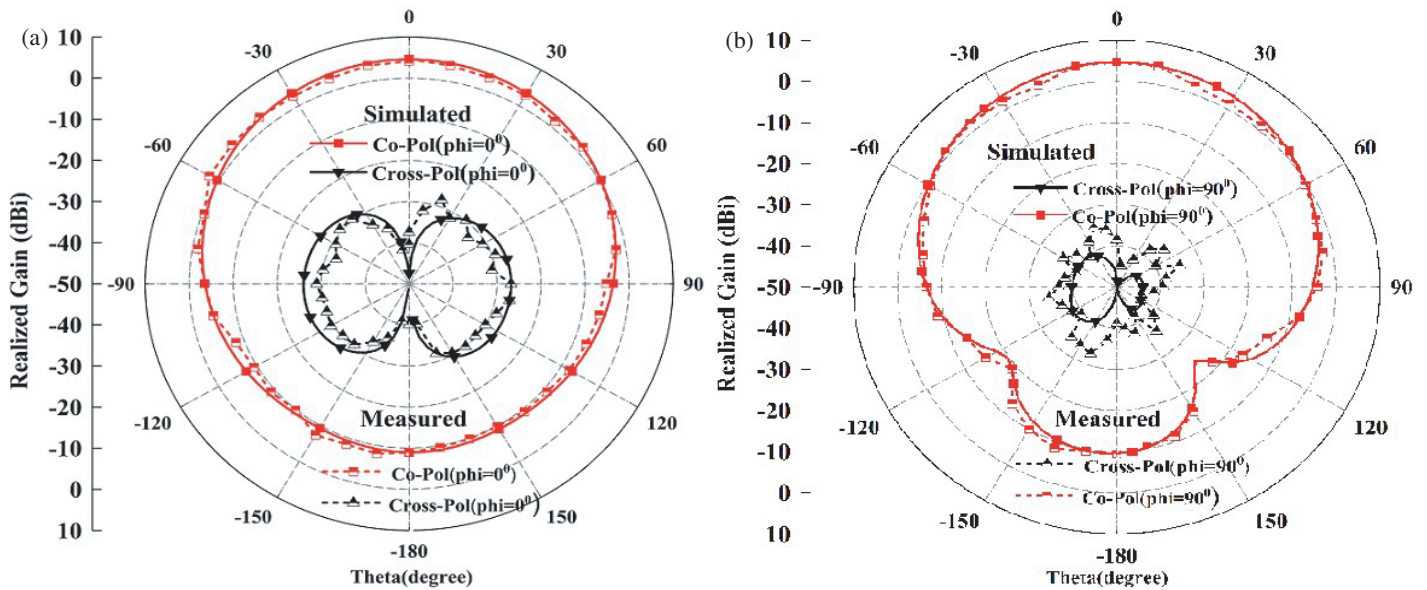


FIGURE 18. The 2-D radiation plots of the suggested design at 5.77 GHz for cloth. (a) $\phi = 0^\circ$, (b) $\phi = 90^\circ$.

read range (R) can be calculated by using Eq. (1) [15, 16].

$$R = \frac{\lambda}{4\pi} \sqrt{\frac{P_r G_r G_t \tau}{P_{\text{threshold}}}} \quad (1)$$

In Eq. (1), λ represents the wavelength; P_r , G_r denotes the reader's power, gain values; G_t denotes the tag's gain; τ represents the maximum value of power coefficient; and $P_{\text{threshold}}$ is the minimum value of threshold power. Read range response can be evaluated with some standard values of the parameters that were chosen such as: $P_r = 10$ dBm, $P_{\text{threshold}} = 0$ dBm, $= 1$, $\tau = 1$, $G_t = 1$ dBi. Fig. 20 shows the read range response of the suggested design evaluated by using Eq. (1). At 5.77 GHz, it shows R_{max} of 2.81 cm. The determined read range

value of the suggested antenna can be helpful in short-range reader applications compared to optical barcodes.

5.3. Comparative Study with Recent Literature

Table 5 compares the proposed design's performance with a few recently published antennas. The constructed antenna offers several distinctive characteristics with reference to its compactness and corresponding gain value. In contrast to the suggested antenna, the designs in [9, 11] have high gain values and large sizes respectively. Similar to this idea, the design in [19] has a comparable gain value but struggles with large size difficulties. The antennas in [17, 20–23] have lower gain values, and the dimension is bigger than the one in the current study. Hence,

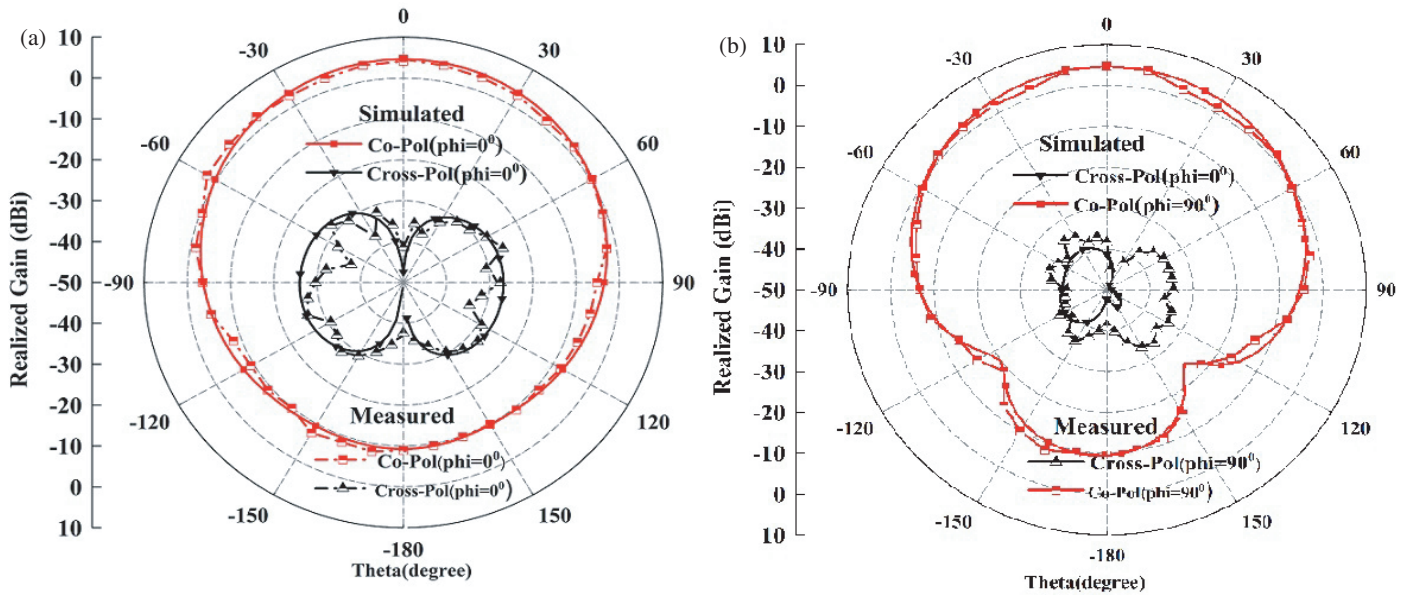


FIGURE 19. The 2-D radiation plots of the suggested design at 5.77 GHz for cardboard. (a) $\phi = 0^\circ$, (b) $\phi = 90^\circ$.

TABLE 5. A comparative study with various LP RFID readers.

| Ref. | Dimension (λ) | -10 dB impedance Bandwidth | f_r (GHz) | Gain (dBi) |
|-----------|--|----------------------------|-------------|------------|
| [9] | $2.50\lambda \times 1.73\lambda \times 0.11\lambda$ | 310 MHz | 5.78 | 5.5 |
| [11] | $0.55\lambda \times 0.55\lambda \times 0.3\lambda$ | 5.89 GHz | 5.8 | 5.1 |
| [18] | $0.78\lambda \times 0.58\lambda \times 0.03\lambda$ | 4.57 GHz | 5.8 | 3.59 |
| [19] | $2.68\lambda \times 2.30\lambda \times 0.03\lambda$ | 0.5–12 GHz | 11.5 | 4.8 |
| [20] | $0.80\lambda \times 0.32\lambda$ | 2.28–2.75 GHz | 2.45 | 4.37 |
| [21] | $0.216\lambda \times 0.292\lambda$ | 2.14–3.35 GHz | 2.45 | 1.85 |
| [22] | $0.22\lambda \times 0.04\lambda \times 0.03\lambda$ | 902–928 MHz | 0.915 | 1.98 |
| [23] | $0.27\lambda \times 0.28\lambda \times 0.008\lambda$ | 860–960 MHz | 0.8665 | 1.39 |
| This Work | $0.43\lambda \times 0.43\lambda \times 0.03\lambda$ | 5.67–5.88 GHz | 5.8 | 4.58 |

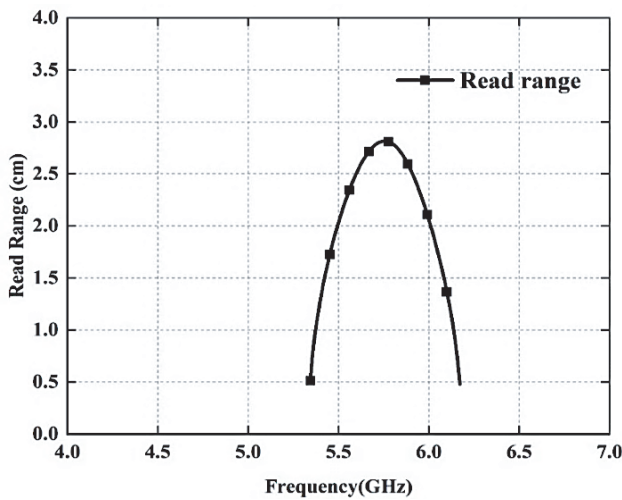


FIGURE 20. The suggested antenna's read range response.

the proposed design is compact and suitable for RFID reader applications.

6. CONCLUSION

An investigation on a linearly polarized hexagonal slot inscribed square-shaped patch antenna has been performed. The prototype was fabricated and measured operating at 5.77 GHz frequency. Analytical modeling is performed to study the operation of the suggested design. The design is verified with the propagation test and found suitable for the usage as a short-range RFID reader with its read range of 2.81 cm and peak achieving a gain of 4.58 dBi at 5.77 GHz. The design has an overall dimension of $0.43\lambda \times 0.43\lambda \times 0.03\lambda$, and in comparison to some current designs, it has been discovered to be compact.

ACKNOWLEDGEMENT

This research is funded by the Fundamental Research Grant Scheme (FRGS) No. Ref: FRGS/1/2022/TK07/UTEM/03/8, provided by Ministry of Higher Education Malaysia (MOHE) and managed by Center for Research and Management (CRIM), Universiti Teknikal Malaysia Melaka (UTeM), Melaka Malaysia.

REFERENCES

- [1] Aslam, B., M. Kashif, M. A. Azam, Y. Amin, J. Loo, and H. Tenhunen, "A low profile miniature RFID tag antenna dedicated to IoT applications," *Electromagnetics*, Vol. 39, No. 6, 393–406, 2019.
- [2] Park, S. and S. Hashimoto, "RFID handbook: Radio-frequency identification fundamentals and applications," *IEICE transactions on fundamentals of electronics, communications and computer sciences*, Vol. 93, No. 4, 711–719, 2010.
- [3] Catarinucci, L., S. Tedesco, and L. Tarricone, "Customized ultra high frequency radio frequency identification tags and reader antennas enabling reliable mobile robot navigation," *IEEE Sensors Journal*, Vol. 13, No. 2, 783–791, 2012.
- [4] Barnard, R., "Innovative RFID applications in the UK," in *The Institution of Engineering and Technology Seminar on RFID and Electronic Vehicle Identification in Road Transport*, Newcastle, UK, Nov. 2006.
- [5] Bhavke, A. and S. Pai, "Advance automatic toll collection & vehicle detection during collision using RFID," in *2017 International Conference on Nascent Technologies in Engineering (ICNTE)*, 1–5, Vashi, India, Jan. 2017.
- [6] Wamba, S. F., A. Anand, and L. Carter, "A literature review of RFID-enabled healthcare applications and issues," *International Journal of Information Management*, Vol. 33, No. 5, 875–891, 2013.
- [7] Mobashsher, A. T., M. T. Islam, and N. Misran, "RFID technology: Perspectives and technical considerations of microstrip antennas for multi-band RFID reader operation," in *Current Trends and Challenges in RFID*, Vol. 7, Cornel Turcu (ed.), IntechOpen, 2011.
- [8] Mobashsher, A. T., M. T. Islam, and N. Misran, "Triple band RFID reader antenna for handheld applications," *Microwave and Optical Technology Letters*, Vol. 53, No. 7, 1629–1632, 2011.
- [9] Bashir, U., K. R. Jha, G. Mishra, G. Singh, and S. K. Sharma, "Octahedron-shaped linearly polarized antenna for multistandard services including RFID and IoT," *IEEE Transactions on Antennas and Propagation*, Vol. 65, No. 7, 3364–3373, 2017.
- [10] Pandav, S., G. Sadhukhan, T. K. Das, S. K. Behera, and M. Mohanty, "Circularly polarized high gain Koch fractal antenna for space applications," *Sādhanā*, Vol. 47, No. 4, 276, 2022.
- [11] Das, T. K., B. Dwivedy, and S. K. Behera, "Design of a meandered line microstrip antenna with a slotted ground plane for RFID applications," *AEU — International Journal of Electronics and Communications*, Vol. 118, 153130, 2020.
- [12] Adriouch, Y., B. Benhmimou, N. Oubahsis, N. Gupta, F. Omari, S. Garg, N. Hussain, I. Najma, R. A. Laamara, and M. E. Bakkali, "Compact and high-gain RFID reader antennas for future internet of things applications," in *Proceedings of Fifth International Conference on Computing, Communications, and Cyber-Security*, 25–34, 2023.
- [13] Nakano, H. and J. Yamauchi, "Printed slot and wire antennas: A review," *Proceedings of the IEEE*, Vol. 100, No. 7, 2158–2168, 2012.
- [14] Garg, R., I. Bahl, and M. Bozzi, *Microstrip Lines and Slotlines*, Artech House, 2013.
- [15] Liu, Q., J. Shen, J. Yin, H. Liu, and Y. Liu, "Compact 0.92/2.45-GHz dual-band directional circularly polarized microstrip antenna for handheld RFID reader applications," *IEEE Transactions on Antennas and Propagation*, Vol. 63, No. 9, 3849–3856, 2015.
- [16] Das, T. K., B. Dwivedy, D. Behera, S. K. Behera, and N. C. Karmakar, "Design and modelling of a compact circularly polarized antenna for RFID applications," *AEU — International Journal of Electronics and Communications*, Vol. 123, 153313, 2020.
- [17] Acharya, A. P., T. K. Das, and T. Shaw, "Design and analysis of compact flower-shaped wideband slotted monopole antenna for RFID reader applications," *AEU — International Journal of Electronics and Communications*, Vol. 169, 154718, 2023.
- [18] Loo, C.-H., K. Elmahgoub, F. Yang, A. Elsherbeni, D. Kajfez, A. Kishk, T. Elsherbeni, L. Ukkonen, L. Sydanheimo, M. Kivikoski, S. Merilampi, and P. Ruuskanen, "Chip impedance matching for UHF RFID tag antenna design," *Progress In Electromagnetics Research*, Vol. 81, 359–370, 2008.
- [19] Mekki, K., O. Necibi, S. Lakhthar, and A. Gharsallah, "A UHF/UWB monopole antenna design process integrated in an RFID reader board," *Journal of Electromagnetic Engineering and Science*, Vol. 22, No. 4, 479–487, 2022.
- [20] Romputtal, A. and C. Phongcharoenpanich, "IoT-linked integrated NFC and dual band UHF/2.45 GHz RFID reader antenna scheme," *IEEE Access*, Vol. 7, 177 832–177 843, 2019.
- [21] Ali, S. H., A. H. Reja, and Y. A. Hachim, "Design of a miniaturized wideband disc monopole antenna used in RFID systems," *Indonesian Journal of Electrical Engineering and Computer Science*, Vol. 21, No. 2, 994–1004, 2021.
- [22] Yan, Y., A. Sharif, J. Ouyang, C. Zhang, and X. Ma, "UHF RFID handset antenna design with slant polarization for IoT and future 5G enabled smart cities applications using CM analysis," *IEEE Access*, Vol. 8, 22 792–22 801, 2020.
- [23] Parthiban, P., "Fixed UHF RFID reader antenna design for practical applications: A guide for antenna engineers with examples," *IEEE Journal of Radio Frequency Identification*, Vol. 3, No. 3, 191–204, 2019.